ENTRANCE CHANNEL DEFORMATION EFFECTS ON SPIN DISTRIBUTIONS OF COMPOUND NUCLEI *,**

K. POMORSKI, W. PRZYSTUPA

Institute of Physics, M. Curie–Skłodowska University
Pl. M. Curie–Skłodowskiej 1, 20-031 Lublin, Poland

AND

J. RICHERT

Physique Théorique, C.R.N. – IN2P3 / Université Louis Pasteur
Strasbourg-Cronenbourg, France

(Received August 28, 1993)

The outcome of the dynamical fission process with prescission particle emission is strongly correlated with the excitation energy and the spin distribution of the initial compound system. We intend to estimate the effect of the deformation of heavy ions in the entrance channel on the spin distribution of the fused system. Classical dynamical calculations with a fluctuating force based on the Langevin equation and one body dissipation have been performed.

PACS numbers: 25.70. -z

1. Introduction

The dynamical description of heavy ion induced fission is strongly correlated with the excitation energy and the spin distribution of the initial fused system. The spin distribution weights the contribution of the set of angular momenta which characterize this system. Hence it is essential to

* Presented at the XXIII Mazurian Lakes Summer School on Nuclear Physics, Piaski, Poland, August 18–28, 1993.

** This work is partly supported by the Polish Committee of Scientific Research under contract No.203119101.

reproduce it properly. In the present work we want to estimate the effect of the deformation of heavy ions in the entrance channel on this distribution in cases for which the experimental distribution is known. We have performed the dynamical calculations with fluctuating force based on the classical Langevin equation [1].

The present paper is the continuation of our previous work [2] and all details of the model are described there. In Section 2 we estimate the limits of the Coulomb barrier between two quadrupole deformed ions corresponding to different geometrical configurations. We develop in Section 3 a simple dynamical fusion model which incorporates in a simplified way the deformation effects and leads to spin distributions of the fused system. Section 4 is devoted to a comparison of these distributions with experimental results obtained for different systems. Conclusions are drawn at the end of the paper.

2. Coulomb barrier between two deformed ions

We have calculated the Coulomb barrier between quadrupole deformed ions for three extreme configurations, see Fig. 1. The barriers are evaluated assuming a square well form for the nuclear potential and they are given by

$$V_c(R) = \frac{Z_1 Z_2 e^2}{R} - \frac{Z_1 e Q_0^{(2)} + Z_2 e Q_0^{(1)}}{4R^3} + \frac{7}{16}\frac{Q_0^{(1)} Q_0^{(2)}}{R^5} \tag{a}$$

$$V_c(R) = \frac{Z_1 Z_2 e^2}{R} + \frac{Z_1 e Q_0^{(2)} + Z_2 e Q_0^{(1)}}{2R^3} + \frac{3}{2}\frac{Q_0^{(1)} Q_0^{(2)}}{R^5} \tag{b}$$

$$V_c(R) = \frac{Z_1 Z_2 e^2}{R} - \frac{Z_1 e Q_0^{(2)} + Z_2 e Q_0^{(1)}}{4R^3} + \frac{11}{48}\frac{Q_0^{(1)} Q_0^{(2)}}{R^5}\,. \tag{c}$$

These expressions are calculated up to the second order in the quadrupole moments $Q_0^{(i)}$, $i = 1, 2$, Z_1 and Z_2 are the proton numbers in the ions and R is the distance between the charge centers of the touching ions. We have assumed here an ellipsoidal shape of the nuclei and the radius constant $r_0 = 1.18$ fm.

The results for the projectile ^{64}Ni and the targets ^{92}Zr, ^{96}Zr and ^{100}Mo are shown in Table I. The estimates of the ground state deformation are taken from [3]. We have evaluated the barriers for the oblate and prolate shapes of ^{96}Zr and ^{100}Mo, because calculations done in [3] predict a small difference between the depths of both minima. The barriers corresponding to the spherical shapes of the colliding nuclei shown in Table I are the reference points. One observes that case (a) is very close to case (c) but a large difference of several MeV is observed between case (a) and case (b).

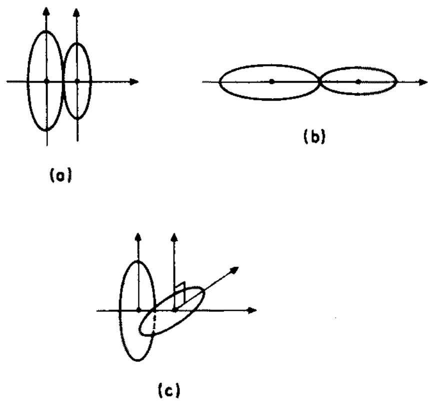

Fig. 1. Configuration for two touching ellipsoids: (a) the axes of symmetry of both fragments are parallel, and perpendicular to the line connecting the mass centers; (b) the axes of symmetry are aligned with the line of centers; (c) the axes of symmetry are perpendicular to each other and to the line connecting both centers.

TABLE I

Coulomb barriers for deformed ions in different configurations as illustrated in Fig. 1. The ground state deformations are taken from Ref. [3].

Reaction	$\epsilon^{(1)}$	$Q_0^{(1)}$	$\epsilon^{(2)}$	$Q_0^{(2)}$	V_c(two sph.)	V_c(a)	V_c(b)	V_c(c)
-	-	b	-	b	MeV	MeV	MeV	MeV
^{64}Ni+^{92}Zr	0.05	0.26	0.00	0.00	160.53	161.42	158.69	161.42
^{64}Ni+^{96}Zr	0.05	0.26	-0.17	-1.47	159.32	156.80	163.57	156.83
^{64}Ni+^{96}Zr	0.05	0.26	0.15	1.52		163.06	151.49	162.99
^{64}Ni+^{100}Mo	0.05	0.26	-0.23	-2.10	166.07	162.19	172.59	162.13
^{64}Ni+^{100}Mo	0.05	0.26	0.18	2.01		170.55	156.56	170.44

This is essentially due to the monopole (first) term in the expression of $V_c(R)$, hence to the distance between the centers of the ions. The estimates in Table I, evaluated in the quadrupole approximation are very close to the exact values obtained using the prescription from Ref. [4]. The maximal error is smaller than 0.3 MeV.

3. Dynamical calculations and spin distributions

In order to get spin distributions of the fused systems we use a classical Langevin equation which we integrate in time over many trajectories up to complete fusion (see *e.g.* [1]). Since an extensive calculation with deformed nuclei with all possible relative orientations is out of scope, we try to estimate the large effects due to deformation, which we observed above, in the following way. We consider the scattering of spherical ions of energy E and, for fixed E, we introduce an energy distribution of gaussian type with the width

$$\Delta E = \delta E + \Delta_1 E + \Delta_2 E\,, \tag{1}$$

where δE is the experimental energy beam width (very small in the case of Van de Graaf accelerators), $\Delta_1 E$ originates from the slow down of the projectile in the target (estimated to be ≤ 1 MeV) and $\Delta_2 E$ is the difference in energy induced by the difference of the Coulomb barriers between the two extreme cases (a) and (b). The average energy of incoming ions is fixed to $E = E_{\rm CM} - \Delta_1 E/2$. In this way we simulate in an approximate way the different fusion barriers induced by the possible deformation of the incoming ions.

The Langevin equations of motion for spherical nuclei, in discretized form, suitable for numerical calculations, can be written in the following form [1]

$$(q_i)_{n+1} = (q_i)_n + \left(\sum_{j=1}^{3} (M)^{-1}_{ij} p_j\right)_n \cdot \tau \tag{2}$$

$$(p_i)_{n+1} = (p_i)_n + \left(\frac{\partial E_k}{\partial q_i} - \frac{\partial V}{\partial q_i} - \sum_{k=1}^{3} \gamma_{ik}\dot{q}_k\right)_n \tau + \sqrt{\tau}\sum_{j=1}^{3} g_{ij}\,\omega_j(\tau)\,, \tag{3}$$

where$\{q_i\} \equiv \{\rho, \lambda, \Delta\}$, $i = 1, 2, 3$ are the shape degrees of freedom and $\{p_i\}$ are the conjugate momenta. The variables ρ, λ and Δ are the relative distance, the neck and the mass asymmetry parameters, respectively [5]. The other parameters in Eqs (2)–(3) have the following meaning: γ_{ik} is the dissipation tensor, M_{ij} is the mass tensor, V is the potential energy, E_k is the kinetic energy and τ is the time step. The last term in Eq. (3) describes the Langevin random force. The matrix g_{ij} is the "square root" of the diffusion tensor [6]

$$D_{ij} = \sum_{k=1}^{3} g_{ik} g_{kj}\,. \tag{4}$$

The quantities ω_j are normally (Gaussian) distributed random variables for the corresponding degrees of freedom.

We assume the Einstein relation between the diffusion and the friction coefficients:

$$D_{ij} = \gamma_{ij}\, T\,, \tag{5}$$

where temperature T is time dependent and is calculated from the dissipated energy E^* along each trajectory. The other set of Langevin equations for the angle of rotation of the whole system Θ, the angles of rotation of the fragments (Θ_1, Θ_2) and for the conjugate momenta [2] has a similar structure as Eqs (2)–(3).

For each trajectory the energy of the incoming ion is chosen randomly taking the gaussian distribution (1) centered around $E_{\rm CM}$ corrected for the slow down in the target. Apart from this point, the calculation leading to fusion events proceeds as usual [1]. In practice, the spin distributions are given by

$$\sigma_l = \left(\frac{d\sigma_F}{dl}\right)_{l_i} = \frac{2\pi}{k^2} l_i \frac{N_i^F}{N_i}, \tag{6}$$

where l_i is the angular momentum, N_i^F is the number of trajectories which, lead to fusion, and N_i is the total number of trajectories with $l = l_i$.

4. Results

The liquid drop potential, the irrotational flow mass and the wall plus window formula were used in the Langevin equations. All the parameters of our model are standard and they are taken from [7].

We have performed calculations for two different systems, ^{64}Ni+^{92}Zr at energy $E_{\rm CM} = 138.8$ MeV and ^{64}Ni+^{96}Zr at $E_{\rm CM} = 139.5$ MeV, for which the spin distributions σ_l have been measured [8, 10]. The results for ^{92}Zr are shown in Fig. 2. The theoretical curves evaluated in our model for three widths, $\Delta E = 0, 1, 2$ and 3 MeV, of the beam energy are compared with the experimental distribution (points) obtained in Ref. [8]. The distributions are renormalized in order to reproduce the total cross section measured in Ref. [9]. It is seen in Fig. 2 that for $\Delta E = 3$ MeV we can reproduce the experimental cross sections for the largest L values. We have got too large cross section for small L values, but it is easy to remove this effect by a small change of the nuclear radius constant r_0 [2].

In Fig. 3, the dependence of σ_F, $\langle L\rangle$ and $\langle L^2\rangle$ on the width of the energy beam is shown. The l.h.s. of the figure represents the results obtained for ^{92}Zr while in the r.h.s. the data for ^{96}Zr are drawn. The total fusion cross sections vary slowly with growing width of the beam energy, while the average value of the angular momentum $\langle L\rangle$ and $\langle L^2\rangle$ of the fused system depends significantly on ΔE. As it was predicted in Table I, one has to use a larger value of ΔE for ^{96}Zr than for ^{92}Zr in order to reproduce the experimental values of $\langle L\rangle$ and $\langle L^2\rangle$.

Similar results as in Fig. 2, but for the reaction ^{64}Ni+^{96}Zr at $E_{\rm CM} = 139.5$ MeV are plotted in Fig. 4. Now, the theoretical curves are obtained in

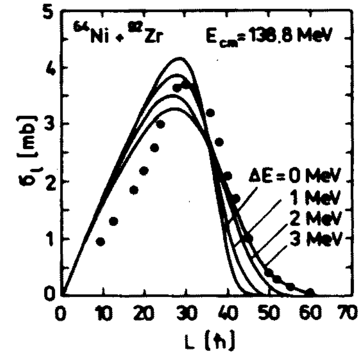

Fig. 2. The cross section $\frac{d\sigma}{dl}$ for the reaction ^{64}Ni+^{92}Zr at $E_{\rm CM} = 138.8$ MeV. The theoretical curves obtained in our model for three values of ΔE are compared with the experimental distribution (points) obtained in Ref. [8]. The distributions are renormalized in order to reproduce the total cross section measured in Ref. [9].

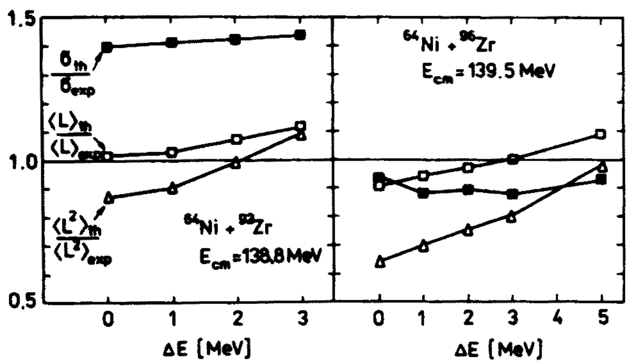

Fig. 3. The dependence of σ_F, $\langle L \rangle$ and $\langle L^2 \rangle$ on the width of the energy beam for two types of targets: ^{92}Zr (l.h.s. of the figure) and ^{96}Zr (r.h.s.).

a simplified model without fluctuating force, which is essentially the same as used in Refs [5, 7], for five widths $\Delta E = 0, 1, \ldots 5$ MeV of the beam energy. The results are compared with the experimental distribution (points) obtained in Ref. [8] It is seen that the final energy width, simulating the effect of different orientation of the projectile and the target nuclei, improves significantly the prediction of σ_L for higher momenta. This result shows that the role of the fluctuating force in Langevin equations could be overestimated in models which do not take the variation of the Coulomb barriers into account.

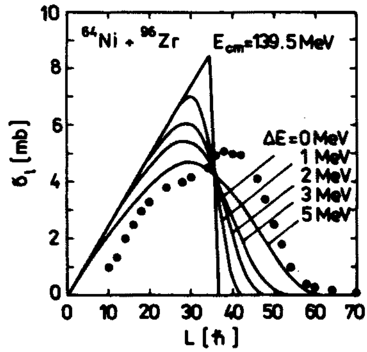

Fig. 4. The cross section $\frac{d\sigma}{dl}$ for the reaction ^{64}Ni+^{96}Zr at $E_{\rm CM} = 139.5$ MeV. The theoretical curves obtained in the model without fluctuating force for five values of ΔE are compared with the experimental distribution (points) obtained in Ref. [8].

5. Summary and conclusions

To summarize, we developed a simple model based on transport concepts in order to work out the fusion cross sections and their dependence on angular momentum. A multi-dimensional Langevin equation was used for the description of heavy ion collisions. The liquid drop potential energy, the hydrodynamical inertia and the one body dissipation with a standard set of parameters, taken from [7], were used. We also relied on the standard Einstein relation in order to estimate the diffusion tensor.

We have reproduced relatively well the partial fusion cross section as a function of the angular momentum. Contrary to our previous estimates made without taking the effect of the deformation into account [2], we have obtained a relatively good agreement also for higher angular momenta. There is no more need to increase the magnitude of the diffusion tensor or the surface friction. Taking into account the effect of fragment deformations on the height of the Coulomb barrier allows the reproduction of the experimental value of the average angular momentum of the fused system and its variance even with a simple model [5, 7] without fluctuating force.

The present model may be improved and refined in several respects. In particular, the relative orientation of the deformed nucleus of the target and of the projectile should be chosen randomly when one fixes the shift of the Coulomb barrier. Our Ansatz with a gaussian distribution of the beam energy can be used to get a rough estimate only.

One of us (K.P.) gratefully acknowledges the warm hospitality extended to him by the Theoretical Physics group of the Centre de Recherches Nucléaires of Strasbourg as well as a grant from the Institut National de Physique Nucléaire et de Physique de Particules (IN2P3). Most of the

numerical calculations were performed on the IBM-9200 computer at the CIUW in Warsaw.

REFERENCES

[1] P. Fröbrich, S.Y. Xu, *Nucl. Phys.* **A477**, 143 (1988); P. Fröbrich, *Nucl. Phys.* **A545**, 87c (1992).
[2] W. Przystupa, K. Pomorski, *Nucl. Phys.* **A** in print.
[3] B. Nerlo-Pomorska, Reports CRN-92-36 and CRN-92-37, 1992, Strasbourg, France; B. Nerlo-Pomorska, K. Pomorski, B. Skorupska-Mach, *Nucl. Phys.* **A** in print.
[4] R.W. Hasse, W.D. Myers, *Geometrical Relationships of Macroscopic Nuclear Physics*, Springer Verlag, 1988.
[5] J. Błocki, H. Feldmeier, W.J. Swiatecki, *Nucl.Phys.* **A459**, 145 (1986).
[6] H. Risken, *The Fokker Planck Equation*, Springer Verlag, 1984.
[7] H. Feldmeier, *Rep. Prog. Phys.* **50**, 915 (1987).
[8] W. Kühn, A. Ruckelshausen, R.D. Fisher, G. Breibach, H.J. Hennrich, V. Metang, R. Novotny, R.V.F. Janssens, T.L. Khoo, D. Habs, D. Schwalm,B. Haas, R.S. Simon, *Phys. Rev. Lett.* **62**, 1103 (1989).
[9] A.M. Stefanini, L. Corradi, H. Moreno, L. Meuller, D.R. Napoli, P. Spolaore, E. Adamides, S. Beghini, G.F. Segato, F. Soramel, C. Signorini, *Phys. Lett.* **252B**, 43 (1990).
[10] A.M. Stefanini, L. Corradi, D. Ackermann, A. Facco, F. Gramegna, H. Moreno, L. Meuller, D.R. Napoli, G.F. Prete, P. Spolaore, S. Beghini, D. Fabris, G. Montagnoli, G. Nebbia, J.A. Ruiz, G.F. Segato, C. Signorini, G. Viesti, *Nucl. Phys.* **A548**, 453 (1992).